Journal of Thermal Analysis and Calorimetry (2019) 135:123–132
https://doi.org/10.1007/s10973-018-7234-7

Study on convective heat transfer and pressure drop of MWCNTs/water nanofluid in mini-tube

Ahmed A. Hussien[1] · Nadiahnor Md Yusop[2] · Mohd Z. Abdullah[3] · Moh'd A. Al-Nimr[4] · Mehrnoush Khavarian[5]

Received: 10 November 2017 / Accepted: 31 March 2018 / Published online: 10 April 2018

Abstract
In recent times, the use of multi-walled carbon nanotubes (MWCNTs)/water nanofluids as a coolant has garnered immense interest due to their high thermal conductivity. Thus, this study investigates the effect of different mass fractions (φ_w) of MWCNTs (0.075, 0.125 and 0.25 mass%) on forced convection heat transfer. Uniform and stable nanofluids were prepared using the two-step method coupled with the addition of water-soluble polymer polyvinyl pyrrolidone (PVP) and using high-power probe sonicator. The test was carried out in a circular mini-tube (D_{in} = 1.1 mm), which was heated uniformly to study the developing and fully developed laminar flow. The Reynolds number (Re) varied from 200 to 500. The heat transfer coefficient was found to be significantly enhanced with increase in mass fraction of MWCNTs in the prepared nanofluid. The maximum enhancement of heat transfer coefficient was 23.9% for the nanofluid prepared with 0.25 mass% of MWCNTs. The experimental result revealed an increase in friction factor using the MWCNTs/water nanofluid. A maximum pressure drop of 9.9% was achieved for the highest mass fraction of MWCNTs.

Keywords MWCNTs · Nanofluids · Heat transfer coefficient · Nusselt number · Thermophysical properties

Introduction

The application of nanofluids as coolant is an emerging method for enhancing the conventional heat transfer fluids. Several studies have been devoted for investigating recent applications of nanofluids in cooling electrical devices, photovoltaic solar cells and mini/micro heat exchangers. Different nanomaterials have been applied in nanofluids such as metallic, oxide metal and carbons family in order to develop the thermophysical properties and enhance the thermal performance of conventional fluids [1–7].

The understanding of the thermophysical properties of nanofluids is important, particularly for forced convective heat transfer. Some studies have focused on the thermophysical properties of various nanofluid materials [8–10]. The main factors influencing the thermophysical properties of nanofluids were shown to be the type of nanomaterial, fraction and size of nanoparticles. Some of the well-known and highly cited conventional correlations used to predict the viscosity and thermal conductivity of nanofluids include Batchelor correlation [11], Brinkman equation [12] and Hamilton and Crosser model [13]. Furthermore, several experimental works have explored the measurement of thermophysical properties [9, 14]. Recently, the application of multi-walled carbon nanotubes (MWCNTs) in forced convective heat transfer is on the rise due to their high thermal conductivity and cylindrical shape, which has further contributed to the remarkable development of the thermophysical properties of base fluids [6, 15].

Numerous studies have explored the thermophysical properties of MWCNTs and contents of the nanocomposite [16, 17]. Some experimental works investigated the effect

✉ Ahmed A. Hussien
ahmed.a.a.hussien@gmail.com

[1] School of Mechanical Engineering, Universiti Sains Malaysia, 14300 Nibong Tebal, Penang, Malaysia

[2] Faculty of Chemical Engineering, Universiti Teknologi MARA, Jalan Ilmu 1/1, 40450 Shah Alam, Selangor, Malaysia

[3] School of Aerospace Engineering, Universiti Sains Malaysia, 14300 Nibong Tebal, Penang, Malaysia

[4] Department of Mechanical Engineering, Jordan University of Science and Technology, Irbid 22110, Jordan

[5] School of Chemical Engineering, Universiti Sains Malaysia, 14300 Nibong Tebal, Penang, Malaysia

of aqueous suspensions of MWCNTs on enhancing heat transfer coefficient. For instance, Ding et al. [18] achieved a significantly enhanced heat transfer coefficient of 350%. Grag et al. [19] studied the laminar convective heat transfer of circular tube using MWCNTs water-based nanofluids. The heat transfer coefficient for 1.0 mass% MWCNTs/water nanofluid was significantly enhanced by approximately 32%. Amrollahi et al. [20] conducted experiments to enhance the heat transfer (via convection) of aqueous fluids containing MWCNTs, with emphasis on the laminar and turbulent flow at the entrance region. The study enhanced heat transfer coefficient by 33 and 40% in laminar and turbulent flows, respectively. The performances of low and high volume fractions of MWCNTs in convective heat transfer and pressure drop were experimentally compared [21]. The maximum enhancements for 0.005 and 0.24% MWCNTs volume fractions were 70 and 190%, respectively. In general, the studies concluded that the enhancement of heat transfer coefficient depends mainly on Reynolds number and fraction of MWCNTs.

The practical aspect of using MWCNTs/water nanofluids to determine the thermal performance of the double-pipe helically coiled heat exchanger was investigated by Wu et al. [22]. No significant effect was found on the low fractions of MWCNTs. However, the effect of MWCNTs on the viscosity of the nanofluids is evidently significant. Sarafraz and Hormozi [23] studied the effect of MWCNTs/water on the heat transfer and pressure drop of a plate heat exchanger. They reported an enhancement in thermal performance of the plate heat exchanger, although higher pressure increase was recorded compared to water. The pressure drop and laminar forced convective heat transfer using MWCNTs water-based nanofluid were investigated experimentally by Hosseinipour et al. [24]. The Reynolds number ranged between 800 and 2000. They noted a significant improvement in heat transfer coefficient with 0.2 mass% of MWCNTs/water nanofluids dispersed using arginine at Re = 2000. Hazbehian et al. [25] have tested the exergy efficiency for 0.1–1.0 vol% of MWCNTs/water nanofluids flow through the circular tube. The range of Reynolds number varied between 800 and 2600. They revealed that the use of nanofluids increased exergy in the range of 22–67%, thus reducing exergy loss in the range of 23–43%. In addition, Estelle et al. [26] studied the thermophysical properties and convective heat transfer of MWCNTs/water nanofluids. They noted enhancement on the heat transfer coefficient up to 11.8%.

Decreasing the hydraulic diameter and increasing the surface area per unit flow volume are very effective ways of removing excess heat [27]. Some recent studies focused on combining the advantages of nanofluid and small channels, for the purpose of obtaining higher single-phase enhancement of heat transfer [28, 29]. The novel application of nanofluids with high thermal conductivity and small channels to enhance heat transfer is still an active area of recent research. For example, Nimmagadda and Venkatasubbaiah [30] experimentally investigated the effect of SWCNTs/water nanofluid on laminar forced convective heat transfer in a wide rectangular microchannel. A significant enhancement in the rate of heat transfer was observed.

The review of aforementioned studies shows there are a lot of efforts to determine the potential usage of aqueous suspensions of MWCNTs in enhancing the forced convective heat transfer. However, the difference in the results was noted since there are very few studies conducted in the area, especially at low Reynolds number and small mass fractions of MWCNTs. In this study, stable and homogeneous MWCNTs/water nanofluids were prepared to study the role of MWCNTs nanomaterial in improving the heat transfer coefficient and pressure drop in mini-tube. In addition, this study also investigated the effect of Reynolds numbers and different mass fractions of MWCNTs.

Materials and nanofluids

Samples preparation

The MWCNTs with a diameter less than 30 nm and a purity of more than 95% were purchased from USAINS Infotech Sdn. Bhd, Malaysia. The MWCNTs were used as received for this experimental study. In the experiment, a uniformly dispersed nanofluid was prepared using the technique suggested by Fadhillahanafi et al. [31] and Sadeghinezhad et al. [32]. The nanofluids were prepared with different MWCNTs fractions of 0.075, 0.125 and 0.25 mass% in distilled water using a two-step method. Firstly, a surfactant was added to MWCNTs/water nanofluids, which was then stirred using a magnetic stirrer at a temperature of 65 °C for 15 min to achieve good dispersion. Polyvinyl pyrrolidone (PVP) water-soluble polymer was selected to improve the stabilization and dispersion of water-repellent MWCNTs in distilled water [33].

In order to obtain well-dispersed MWCNTs, the solution was sonicated using a high-power probe sonicator (SG-24-500P, Telsonic Ultrasonics, 18.4 kHz). It should be mentioned that the solution was placed in an ice bath to prevent any overheating and over bubbling. The homogeneity of the solution was examined every 5 min by pouring a drop of solution into 50 mL distilled water. The nanofluids were fully dispersed if the dropping diffused fast and homogeneously. High uniformity and homogeneity were noted after 15 min of sonication. The pH values were measured for all nanofluids with different MWCNTs mass fractions.

Values of pH are about 6.5. Figure 1 shows the stability of different mass fractions of MWCNTs/water nanofluids dispersed for more than 6 months.

MWCNTs characterization and stability

Field emission scanning electron microscopy (FESEM; Supra-35VP) was used to characterize the morphology, nanotube size and the purity of the MWCNTs. The cylindrical cross-bundles of MWCNTs are observable in Fig. 2. Measuring the accurate length of the MWCNTs from FESEM observation is rather difficult because of the twisting morphology.

XRD was performed to investigate the structure of MWCNTs. X-ray diffraction (XRD) patterns were obtained using a Philips XRD machine at a scanning rate of 0.015 °/s. In a typical experiment, 30 mg of catalyst was placed in a U-shape quartz tube, degassed with a 50 cm^3/min stream of N_2 at 150 °C for 1 h to remove traces of water, and then cooled to ambient temperature. The XRD spectrum of the MWCNTs is shown in Fig. 3. The XRD diffraction peaks are observed at 26.5°, 42.4° and 63.6°, which correspond to the hexagonal graphite structure of C (002), C (100) and C (110), respectively [34].

Thermogravimetric analysis (TGA) and differential thermal analysis (DTA) were performed using an SDT Q600 TA instrument. TGA–DTA analysis was used to estimate the thermal stability of MWCNTs. The DTA and TGA curves of MWCNTs are presented in Fig. 4. Based on the TGA result, the main mass loss region at the temperature between 400 and 710 °C corresponds to the oxidation of MWCNTs. According to the DTA curve, the main thermal event peak occurs at approximately 614 °C, which can be attributed to the high thermal stability of MWCNTs [35].

Experimental setup

In order to evaluate the heat transfer coefficient and pressure drop of MWCNTs/water nanofluids, an experiment was designed as illustrated in Fig. 5a. The experimental setup consists of a fluid reservoir, pump, test section and cooling unit. Figure 5b shows the test section, which is a

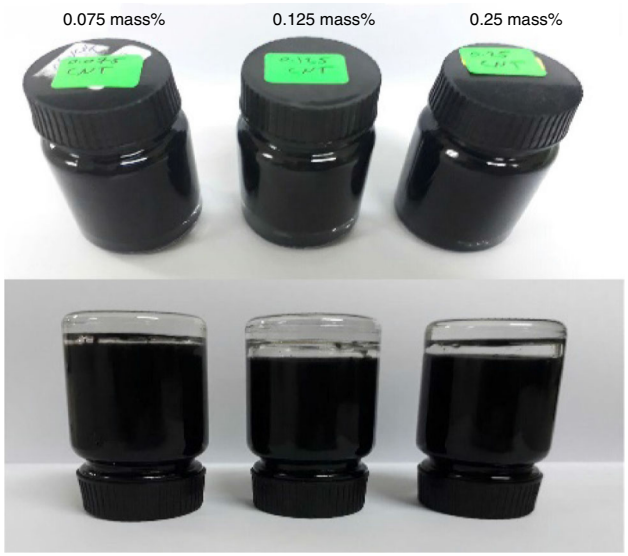

Fig. 1 Photograph of MWCNTs/water nanofluids after over 6 months of dispersion

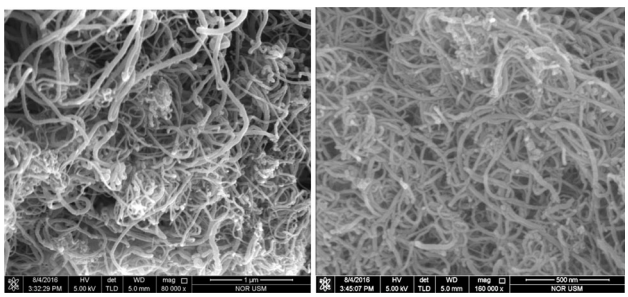

Fig. 2 FESEM images of MWCNTs at different magnifications

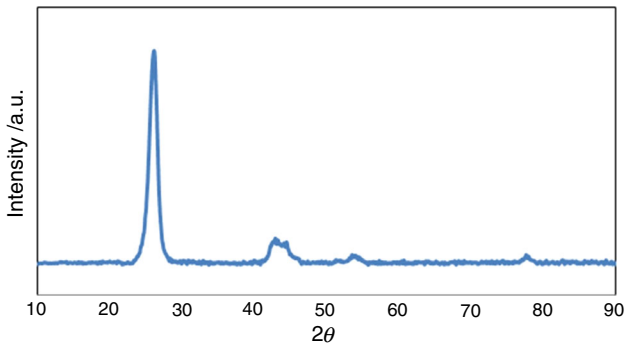

Fig. 3 XRD pattern of MWCNTs

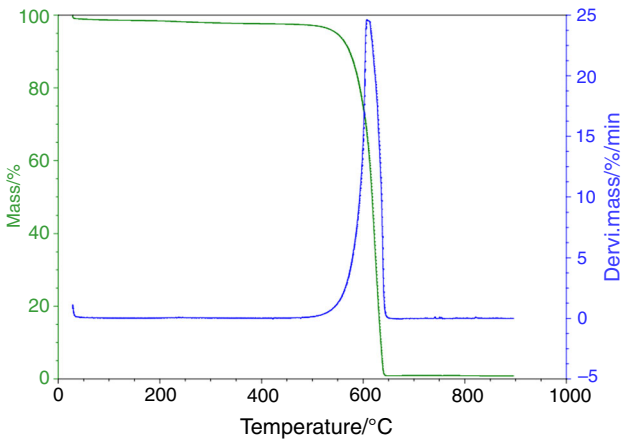

Fig. 4 DTA and TGA curves of MWCNTs

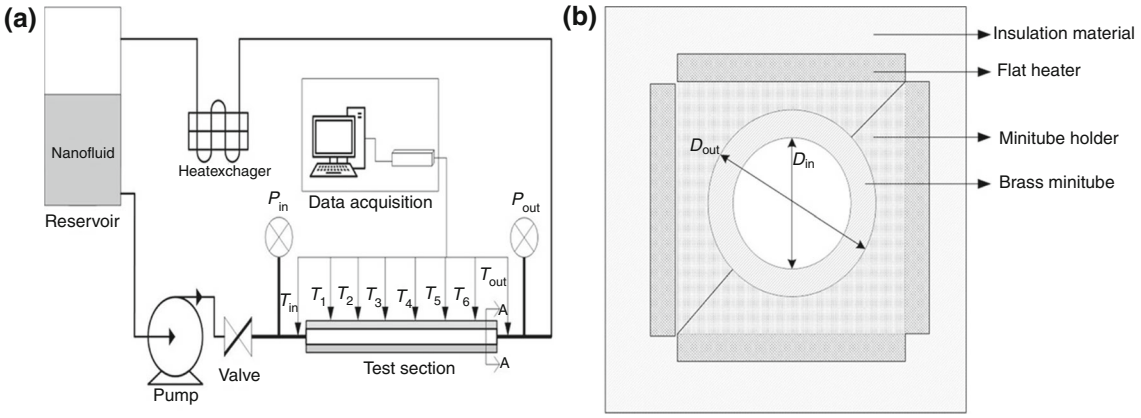

Fig. 5 **a** Schematic diagram of experimental setup and **b** A–A section of test section

brass mini-tube with inner diameter of 1.1 mm, total length of 270 mm and wall thickness of 0.45 mm. This tube was held inside a stainless steel mini-tube holder, which was fabricated to serve the uniformity heat flux of the boundary condition. Four electrical flat heaters (20 W) were fixed on the four sides of the mini-tube holder. The heat sink compound was used to fill the clearance between the stainless steel holder and mini-tube to make a better and consistent contact. To minimize the heat lost to the surrounding, many layers of high-quality woven fiberglass with a total thermal insulation thickness of 35 mm were utilized.

The measurement of the inlet pressure was indicated by a digital pressure indicator (0–700 bar, DPI-705, Druck Ltd., UK). Six thermocouples (K-type) were attached the outer wall of the mini-tube using thermal adhesive to measure the temperature at different axial locations (Z = 43, 75, 119, 160, 206 and 230 mm). The measured temperatures were reported as T_1, T_2, T_3, T_4, T_5 and T_6 according to the distance from the inlet. Furthermore, two other thermocouples were used to measure the temperature of nanofluids (T_{in} and T_{out}) at the inlet and outlet of mini-tube.

Data processing

Thermophysical properties of nanofluids

The general formula used to compute the density and specific heat for nanofluids is a classical two-phase mixture, as shown in Eqs. 1 and 2:

$$\rho_{nf}(T) = (1-\varphi_v)\rho_{bf}(T) + \varphi_v\rho_{np} \quad (1)$$

$$(c_p\rho)_{nf}(T) = (1-\varphi_v)(c_p\rho)_{bf} + \varphi_v(c_p\rho)_{np} \quad (2)$$

where φ_v denotes the volume fraction of MWCNTs. The calculation used to convert from mass fraction (φ_w) to volume fraction is presented in Eq. 3:

$$\varphi_v = \frac{\varphi_w\rho_{bf}}{\rho_p + \varphi_w\rho_{bf} - \varphi_w\rho_p} \quad (3)$$

The viscosity of nanofluids was computed using the Batchelor correlation, with the effect of temperature taken into consideration [11]. Although this equation is principally used for spherical particles with volume fractions less than 5.0 vol%, it can also be used for other particle shapes with low volume fractions such as MWCNTs according to [8, 36, 37].

$$\mu_{eff}(T) = \left(1 + 2.5\varphi_v + 6.2\varphi_v^2\right)\mu_{bf}(T) \quad (4)$$

To predict the thermal conductivity of nanofluids, this study adopted the correlation equation by Hamilton and Crosser model shown in Eq. 5, which was found to be compatible with experimental data for $\varphi_v < 30\%$ [13, 21, 38]:

$$k_{eff}(T) = k_{bf}(T)\frac{k_p + (n-1)k_{bf}(T) + (n-1)\left(k_p - k_{bf}(T)\right)\varphi_v}{k_p + (n-1)k_{bf}(T) - \left(k_p - k_{bf}(T)\right)\varphi_v} \quad (5)$$

where n denotes the shape factor, which is obtained from experimental shape coefficient. The shape factor values (n) for spherical and cylindrical particles are 3 and 6, respectively.

However, for low fractions of nanofluids, Duangthongsuk, Wongwises [36] reported an insignificant difference in heat transfer coefficient for different conventional models used to predict the thermophysical properties of nanofluids.

Heat transfer

Heat loss is the deviation between the supplied energy to the electrical flat heaters, and the absorbed energy in the working fluids, which can be computed using Eq. 6:

$$\emptyset_{loss} = \frac{VI - \dot{m}c_p(T_{out} - T_{in})}{VI} \times 100\% \quad (6)$$

The maximum heat loss was found to be 5.6%, which is possibly due to the significant variance between the ambient temperature and the test section, which could reach up to 60 °C.

The heat transfer performance of flowing nanofluids was based on convective heat transfer coefficient (h) and the Nusselt number (Nu) [39]:

$$h(Z) = \frac{q}{(T_{\mathrm{wi}}(Z) - T_{\mathrm{f}}(Z))} \tag{7}$$

$$Nu(Z) = h(Z)D_{\mathrm{in}}/k_{\mathrm{nf}} \tag{8}$$

where q denotes the heat flux, which can be calculated from the heat gain (absorbed) by the working fluid:

$$q = \rho_{\mathrm{nf}} c_{\mathrm{pnf}} u(T_{\mathrm{in}} - T_{\mathrm{out}}) \tag{9}$$

k_{nf} signifies the thermal conductivity of the nanofluid, and $T_{\mathrm{wi}}(Z)$ represents the inner wall temperature at Z axial distance from the entrance, which can calculated by applied radial heat conduction equation (Eq. 10):

$$T_{\mathrm{wi}}(Z) = T_{\mathrm{wo}}(Z) + \frac{q ln\left(\frac{D_{\mathrm{o}}}{D_{\mathrm{i}}}\right)}{2\pi l k_{\mathrm{s}}} \tag{10}$$

where l and k_{s} are the total length and thermal conductivity of the mini-tube material, respectively. The surface wall temperature of mini-tube $T_{\mathrm{wo}}(Z)$ was measured at different axial locations ($^{Z}/_{D}$ = 39, 68, 108, 145, 187 and 209). The mean fluid temperatures (T_{f}) were obtained at an axial distance from the entrance through the energy balance with zero heat loss, as shown in Eq. 11:

$$T_{\mathrm{f}}(Z) = T_{\mathrm{in}} + q\pi D_{\mathrm{i}} Z/\left(\rho_{\mathrm{nf}} c_{\mathrm{p,nf}} uA\right) \tag{11}$$

where nanofluid properties were evaluated at a mean temperature (T_{m}):

$$T_{\mathrm{m}} = (T_{\mathrm{in}} + T_{\mathrm{out}})/2 \tag{12}$$

The local Nusselt numbers (Nu) in a round tube with uniform heat flux can be presented by Eq. 13 [40]:

$$Nu = \begin{cases} 1.953 Z^{*\frac{1}{3}} & Z^* \geq 33.33 \\ 4.364 + 0.0722 Z^* & Z^* \leq 33.33 \end{cases} \tag{13}$$

where $Z^* = RePr\left(\frac{D_{\mathrm{in}}}{Z}\right)$ and $Pr = \frac{c_{\mathrm{p,nf}}\mu_{\mathrm{nf}}}{k_{\mathrm{nf}}}$.

Pressure drop

The theoretical friction factor values of a fully developed laminar flow were determined using Hagen–Poiseuille equation, as shown in Eq. 14:

$$f = \frac{64}{Re} \tag{14}$$

The theoretical values were compared with measured results of Δp by applying the Darcy friction factor (f), which is defined in Eqs. 15 and 16 as:

$$f = 2\frac{(\Delta p/l)D_{\mathrm{i}}}{\rho_{\mathrm{nf}} u^2} \tag{15}$$

$$\Delta p = 32\frac{u\mu l}{D_{\mathrm{i}}^2} \tag{16}$$

The mean velocity can be calculated from the flow rate Q and mini-tube cross-sectional area A (Eq. 17):

$$u = Q/A \tag{17}$$

Uncertainty analysis

The uncertainty error of experimental apparatuses (bias error) is a systematic and constant error that arises during the experiments. Table 1 shows the uncertainties of the experimental apparatus. The estimated uncertainties were calculated using the mean values of the measured parameters. The average measurement uncertainties of pressure, volume and temperature are 5.1, 1.2 and 0.58%, respectively. This precision error can be attributed to the deviation of repeated measurements from the mean and the number of iterated values. The errors derived from mass flow rate, Reynolds number, heat transfer coefficient and friction factor parameters can be identified using the root sum square method [41]. The maximum error calculations of Reynolds number, heat transfer coefficient and friction factor are 2.3, 4 and 2.4%, respectively.

Results and discussions

The measured Reynold numbers varied from 200 to 500, which indicates that the bulk velocities range between 0.1 and 0.3 m/s for the tested nanofluids. The mini-tube outer surface was exposed to 10600 W/m^2 heat flux. It was calculated by determining the voltage and the current supplied to the flat heaters. Distilled water was utilized as the benchmark sample to validate the experimental rig at

Table 1 Uncertainties of the experimental apparatus

Apparatus	Uncertainty
K-type thermocouples	± 0.18 °C
Balance	± 0.0001
AC source	± 3 V
Timer	± 0.01 s
Collecting beaker	± 2 mL
Pressure transducer	± 7 pa

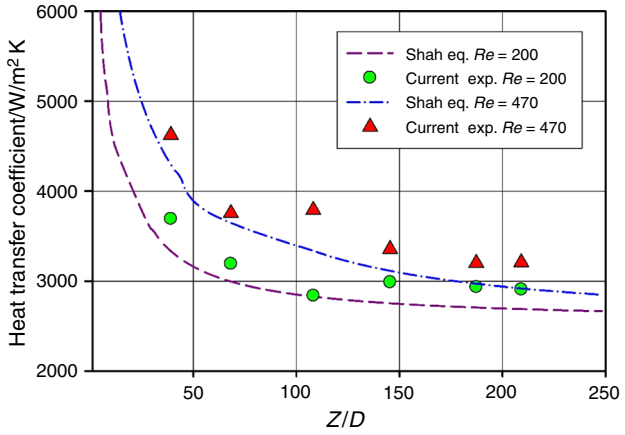

Fig. 6 Experimental validation using distilled water

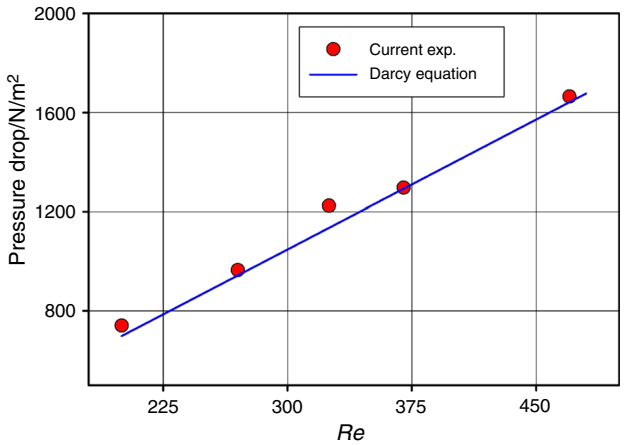

Fig. 7 Variation of pressure drop with Reynolds number for distilled water

two different Reynolds numbers. The validation of experimental setup was performed based on the Shah equation [40], as shown in Fig. 6.

The measurement of pressure drop variation with Reynolds number for distilled water (Fig. 7) was carried out to determine the accuracy of the experimental setup. It can be observed that the difference between calculated pressure drop from Eq. 16 and measured pressure drop data is less than 5%. The results of mini-tube pressure drop at laminar flow regime are consistent with the Darcy equation (Eq. 16), which suggests that the conventional theories are valid for forced convective heat transfer using small tubes [29, 42]. The slightly greater measured pressure drop compared with theoretical values might be due to minor head loss such as T-connection, pipe entrance or exit and sudden expansion or contraction.

The effect of the MWCNTs/water nanofluids on the measured mini-tube wall temperature for inlet fluid temperature of 27 °C is presented in Fig. 8. The results

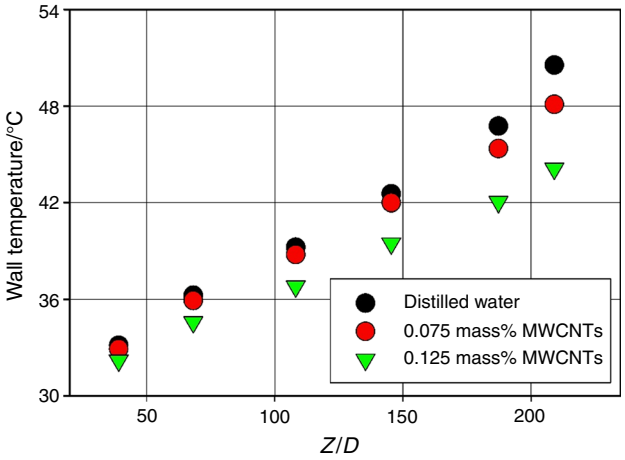

Fig. 8 Wall temperature at different axial locations (Re = 470)

revealed that the use of distilled water induced higher wall temperature compared with nanofluids. Thus, it can be inferred that the MWCNTs/water nanofluids have the ability to improve the heat transfer rate. The wall temperature depends on MWCNTs mass fractions, Reynolds numbers and axial location.

Figure 9a–c illustrates the effect of the mass fractions of MWCNTs on local heat transfer coefficient at different Re numbers of 200, 325 and 470, respectively. The heat transfer coefficient increased proportionately with the mass fraction of MWCNTs. As shown in Fig. 9a at Re = 200, the relative enhancement of the heat transfer coefficients in average was 5.5, 13.1 and 23.9% for MWCNTs fraction of 0.075, 0.125 and 0.25 mass%, respectively. This percentage is calculated using Eq. 18:

$$h_{\text{enhanc.}}\% = \frac{(h_{\text{nf}}(Z) - h_{\text{water}}(Z))}{h_{\text{water}}(Z)} \times 100\% \tag{18}$$

Furthermore, the results showed the importance of MWCNTs fractions in improving heat transfer. The average heat transfer coefficient at Re of 325 was 3.6, 10.4 and 18.4% for MWCNT nanofluid fractions of 0.075, 0.125 and 0.25 mass%, respectively, as shown in Fig. 9b. Also, an inverse relation was observed between Reynolds number and developing heat transfer. For instance, the average enhancement of heat transfer coefficient at Re = 200, Re = 325 and Re = 470 with MWCNTs mass fraction of 0.125 mass% was 13.1, 10.4 and 8.7%, respectively. The enhanced heat transfer coefficient is due to the development of thermophysical properties of nanofluids [43]. Other factors that contribute to enhancing heat transfer using nanofluids include Brownian motion and shape of the nanoparticles [7]. However, Ding et al. [18] attributed the significant enhancement in heat transfer coefficient to increase in the Peclet number, resulting from the shape of CNTs. The enhancement of heat transfer coefficient is also

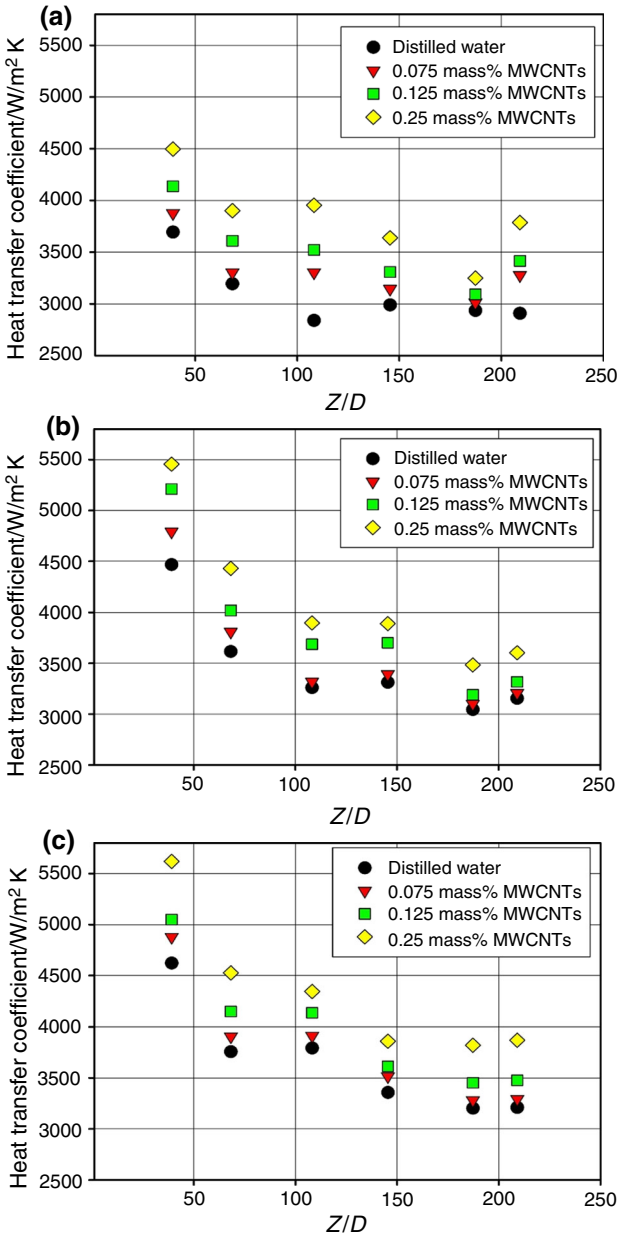

Fig. 9 Effect of different fractions of MWCNTs on axial heat transfer coefficient at **a** Re = 200, **b** Re = 325 and **c** Re = 470

relatively dependent on the axial location. However, unlike water, the local heat transfer coefficient of MWCNTs/water nanofluids dropped at the end of the mini-tube. As shown in Fig. 9, the enhancement of heat transfer at the entrance was the highest. However, such condition did not assure that the enhancement was less than the average at the end of the tube. This phenomenon was reported in a previous study [18].

The average enhancement occurred when the nanofluids were at the developing region of the tube. At Re = 325, the local enhancement of heat transfer coefficient of 0.125 mass% nanofluid at Z = 43 mm was 16.7%, with an average of 10.4%. Similarly, the local enhancement of heat transfer coefficient at the same axial location (Z = 43 mm) for a different mass fraction (0.25 mass%) and Reynolds number (Re = 470) was 21.5% with an average of 18.6% compared to water. In addition to the increase in thermal conductivity of nanofluids, one of the foremost causes of the entrance effect of nanofluids is their thermophysical properties, which increased the thermal developing length. For instance, at Re = 200 and 0.25 mass% nanofluid, the thermal entrance length increased by 3 mm. Also, the Brownian motion and thermophoresis forces become efficient at the high-temperature gradient in the developing region [44]. These results are consistent with reports that mini-tube positively affects heat transfer coefficient [45].

The deductions from the results are based on the predicted values of thermal conductivity and viscosity of nanofluid, which in turn are based on theoretical formulas of temperature effect. Many studies have confirmed that the measured thermal conductivity is much higher than predicted by the theoretical relations [22, 38]. The experimental results of the MWCNTs/water nanofluid for laminar flow showed a maximum enhancement of 23.9% in heat transfer coefficient at Re = 200 compared with the base fluid. The effect of axial heat conduction at mini-tube wall might significantly affect the enhancement of heat transfer coefficient at the entrance of tube length. Yang and We [46] stated in their numerical research that the effect of wall thickness on axial heat conduction is higher at the entrance region. The maximum axial heat conduction is near the inlet of mini-tube and minimum in the flow direction. The impact of axial wall conduction of mini-tube on heat transfer coefficient is high (Fig. 9), due to the influence of conjugated heat transfer at low Reynolds number [47]. In this regard, the variation between the local heat transfer coefficients was more significant.

Figure 10 shows the effect of Reynolds number on the average heat transfer coefficient enhancement at different mass fractions of MWCNTs. Theoretically, the heat transfer coefficient of MWCNTs increases with an increase in mass flow rate, but slightly higher for water. Figure 10 shows that average heat transfer coefficient increases linearly with Reynolds number (Re). Heat transfer enhancement increased with increasing mass fractions. The effect of mass fractions of MWCNTs on average heat transfer coefficient is observed to be the highest at the lowest Reynolds number, and vice versa. At Re = 200, the average heat transfer coefficient was enhanced by 5.5, 13.1 and 23.9% for 0.075, 0.125 and 0.25 mass%, respectively. In addition, the average heat transfer was enhanced by 3.7, 8.7 and 18.6% for Re = 470. A similar trend of negative effect of Reynolds number on the enhancement of heat transfer coefficient was reported by Ding et al. [18] and Grag et al.

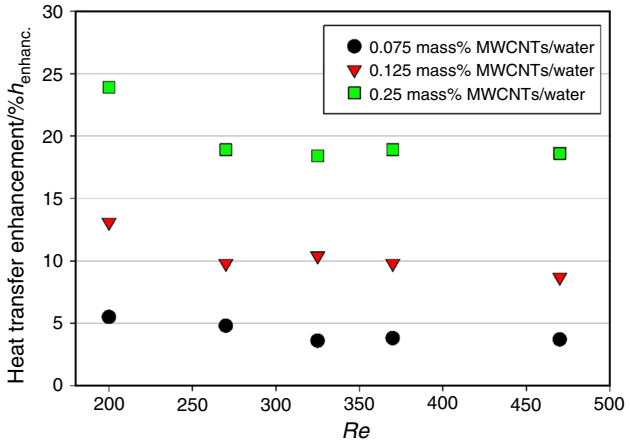

Fig. 10 Effect of different Reynolds numbers on average heat transfer coefficient enhancement for different fractions of MWCNTs

[19], although for different Reynolds numbers and tube diameters.

The effect of MWCNTs present in base fluids on the improvement in Nusselt number can be understood through combinations of thermophysical properties (Peclet number). Peclet number is defined as $Pe = RePr$. The variation in average Nusselt number with Peclet number for different mass fractions of MWCNTs is presented in Fig. 11. This figure reveals the effect of Peclet number and mass fractions of MWCNTs on enhancing the Nusselt number of base fluid. As the Peclet number increased from 750 to 2360 and the mass fraction of MWCNTs increased from 0.075 to 0.25 mass%, the average Nusselt number concomitantly increased from 5.61 to 6.66 and 6.55 to 7.6, respectively. Therefore, it can be inferred that convective heat transfer is enhanced with greater mass fraction of MWCNTs.

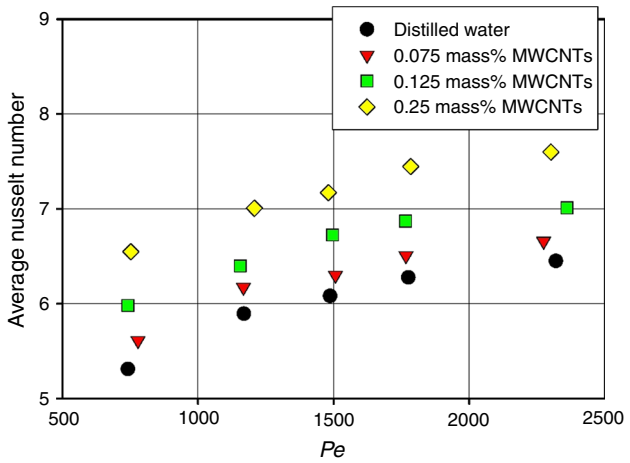

Fig. 11 Variation of average Nusselt number with Peclet number for different mass fractions of MWCNTs

In addition to the heat transfer enhancement, increase in pumping power is also crucial, particularly in the industrial application of nanofluids. Increase in pumping power is a major obstacle in the application of nanofluids due to the existing pressure drop [6]. Hence, this study performed an experiment to find the pressure drop of MWCNTs/water nanofluids compared with the theoretical results.

The relationship between pressure drop and friction factor for various fractions of MWCNTs at different Reynolds numbers is shown in Figs. 12 and 13, respectively. The friction factors for different fractions of MWCNTs/water nanofluid were slightly higher than that of pure water. The Reynolds number increases as the friction factor decreases. Furthermore, the low Reynolds number created the maximum pressure drop of nanofluids compared with the base fluid, as shown in Fig. 12. Thus, the higher friction factor influenced the increase in the nanofluids fraction. The increased mass fractions of MWCNTs indicate increase in the viscosity of nanofluid, because the nanomaterials in fluids easily form agglomerations and clusters

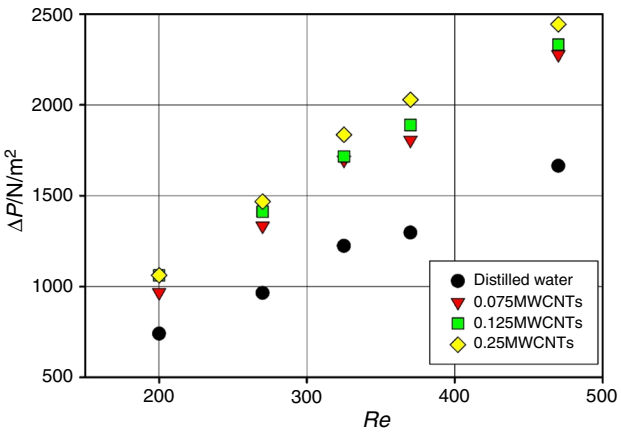

Fig. 12 Effect of different fractions of MWCNTs on pressure drop

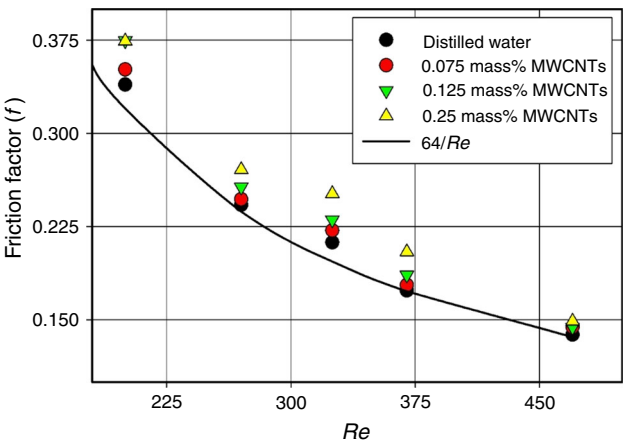

Fig. 13 Effect of different fractions of MWCNTs on friction factor

in addition to undergoing surface adsorption. The average increase in friction factor of 0.075 mass% MWCNTs/water nanofluid over base fluid was 1.8%. However, the increasing of friction factor of 0.25 mass% MWCNTs/water nanofluid in average was 9.9% over base fluid. The significant difference in friction factor is possibly due to the greater size of the MWCNTs (in microns) compared with other nanoparticles material or the random movements of the MWCNTs. The 25% increase in pressure drop has been earlier reported by Wang et al. [21]. Thus, the use of low fractions of MWCNTs is recommended to reduce the possibility of pressure drop [24].

The friction factor values were correlated with Reynolds number and different mass fractions of MWCNTs using MATLAB nonlinear polynomial curve fitting, which is as follows:

$$f(Re,\emptyset) = 0.681 - 0.00215Re + 2.107 \times 10^{-6}Re^2 + 0.1285\emptyset - 0.0001294Re\emptyset \quad (19)$$

The predicted correlation is consistent with the experimental results shown in Fig. 13. The R-square and RMSE are 0.9927 and 0.006998, respectively.

Conclusions

This research applies MWCNTs/water nanofluids with small tubes to improve convective heat transfer. In this regard, constant heat flux with fully laminar flow (Re = 200–500) was applied as boundary conditions. The thermal conductivity and the viscosity of the MWCNTs/water nanofluids were predicted based on a theoretical model that accounts for the fundamental role of Brownian motion and temperature contours. Different mass fractions of MWCNTs (0.075, 0.125 and 0.25 mass%) were prepared using a two-step method with a very low fraction of polyvinyl pyrrolidone (PVP) as dispersant. The results showed enhancement of laminar convective heat transfer coefficients with the use of the MWCNTs. The average enhancement of heat transfer coefficient increases proportionately with the fraction of MWCNTs, but decreases with the Reynolds number. The maximum enhancement of heat transfer coefficient was 23.9% at 0.25 mass% of MWCNTs/water nanofluid and Reynolds number (Re) of 200. The friction factor was also found to increase with the use of MWCNTs/water nanofluids.

Acknowledgements The first author would like to thank to Universiti Sains Malaysia fellowship for financial support to this article.

References

1. Hussien AA, Abdullah MZ, Moh'd AA-N. Single-phase heat transfer enhancement in micro/minichannels using nanofluids: theory and applications. Appl Energy. 2016;164:733–55.
2. Ganvir R, Walke P, Kriplani V. Heat transfer characteristics in nanofluid: a review. Renew Sustain Energy Rev. 2017;75:451–60.
3. Hwang Y, Ahn Y, Shin H, Lee C, Kim G, Park H, et al. Investigation on characteristics of thermal conductivity enhancement of nanofluids. Curr Appl Phys. 2006;6(6):1068–71.
4. Pradhan N, Duan H, Liang J, Iannacchione G. The specific heat and effective thermal conductivity of composites containing single-wall and multi-wall carbon nanotubes. Nanotechnology. 2009;20(24):245705.
5. Baghbanzadeh M, Rashidi A, Soleimanisalim AH, Rashtchian D. Investigating the rheological properties of nanofluids of water/hybrid nanostructure of spherical silica/MWCNT. Thermochim Acta. 2014;578:53–8.
6. Yazid MNAWM, Sidik NAC, Yahya WJ. Heat and mass transfer characteristics of carbon nanotube nanofluids: a review. Renew Sustain Energy Rev. 2017;80:914–41.
7. Kleinstreuer C, Feng Y. Experimental and theoretical studies of nanofluid thermal conductivity enhancement: a review. Nanoscale Res Lett. 2011;6(1):229.
8. Baratpour M, Karimipour A, Afrand M, Wongwises S. Effects of temperature and concentration on the viscosity of nanofluids made of single-wall carbon nanotubes in ethylene glycol. Int Commun Heat Mass Transf. 2016;74:108–13.
9. Indhuja A, Suganthi K, Manikandan S, Rajan K. Viscosity and thermal conductivity of dispersions of gum arabic capped MWCNT in water: influence of MWCNT concentration and temperature. J Taiwan Inst Chem Eng. 2013;44(3):474–9.
10. Azmi W, Sharma K, Mamat R, Najafi G, Mohamad M. The enhancement of effective thermal conductivity and effective dynamic viscosity of nanofluids: a review. Renew Sustain Energy Rev. 2016;53:1046–58.
11. Batchelor G. The effect of Brownian motion on the bulk stress in a suspension of spherical particles. J Fluid Mech. 1977;83(01):97–117.
12. Brinkman H. The viscosity of concentrated suspensions and solutions. J Chem Phys. 1952;20(4):571.
13. Hamilton R, Crosser O. Thermal conductivity of heterogeneous two-component systems. Ind Eng Chem Fundam. 1962;1(3):187–91.
14. Sadri R, Ahmadi G, Togun H, Dahari M, Kazi SN, Sadeghinezhad E, et al. An experimental study on thermal conductivity and viscosity of nanofluids containing carbon nanotubes. Nanoscale Res Lett. 2014;9(1):1–16.
15. De Volder MF, Tawfick SH, Baughman RH, Hart AJ. Carbon nanotubes: present and future commercial applications. Science. 2013;339(6119):535–9.
16. Esfe MH, Saedodin S, Mahian O, Wongwises S. Thermophysical properties, heat transfer and pressure drop of COOH-functionalized multi walled carbon nanotubes/water nanofluids. Int Commun Heat Mass Transf. 2014;58:176–83.
17. Halelfadl S, Estellé P, Aladag B, Doner N, Maré T. Viscosity of carbon nanotubes water-based nanofluids: influence of concentration and temperature. Int J Therm Sci. 2013;71:111–7.
18. Ding Y, Alias H, Wen D, Williams RA. Heat transfer of aqueous suspensions of carbon nanotubes (CNT nanofluids). Int J Heat Mass Transf. 2006;49(1):240–50.
19. Garg P, Alvarado JL, Marsh C, Carlson TA, Kessler DA, Annamalai K. An experimental study on the effect of ultrasonication on viscosity and heat transfer performance of multi-wall

carbon nanotube-based aqueous nanofluids. Int J Heat Mass Transf. 2009;52(21):5090–101.
20. Amrollahi A, Rashidi A, Lotfi R, Meibodi ME, Kashefi K. Convection heat transfer of functionalized MWNT in aqueous fluids in laminar and turbulent flow at the entrance region. Int Commun Heat Mass Transf. 2010;37(6):717–23.
21. Wang J, Zhu J, Zhang X, Chen Y. Heat transfer and pressure drop of nanofluids containing carbon nanotubes in laminar flows. Exp Thermal Fluid Sci. 2013;44:716–21.
22. Wu Z, Wang L, Sundén B, Wadsö L. Aqueous carbon nanotube nanofluids and their thermal performance in a helical heat exchanger. Appl Therm Eng. 2016;96:364–71.
23. Sarafraz M, Hormozi F. Heat transfer, pressure drop and fouling studies of multi-walled carbon nanotube nano-fluids inside a plate heat exchanger. Exp Thermal Fluid Sci. 2016;72:1–11.
24. Hosseinipour E, Heris SZ, Shanbedi M. Experimental investigation of pressure drop and heat transfer performance of amino acid-functionalized MWCNT in the circular tube. J Therm Anal Calorim. 2016;124(1):205–14.
25. Hazbehian M, Mohammadiun M, Maddah H, Alizadeh M. Analyses of exergy efficiency for forced convection heat transfer in a tube with CNT nanofluid under laminar flow conditions. Heat Mass Transf. 2017;53(5):1503–16.
26. Estellé P, Halelfadl S, Maré T. Thermophysical properties and heat transfer performance of carbon nanotubes water-based nanofluids. J Therm Anal Calorim. 2017;127(3):2075–81.
27. Tuckerman DB, Pease R. High-performance heat sinking for VLSI. IEEE Electron Device Lett. 1981;2(5):126–9.
28. Khoshvaght-Aliabadi M, Pazdar S, Sartipzadeh O. Experimental investigation of water based nanofluid containing copper nanoparticles across helical microtubes. Int Commun Heat Mass Transf. 2016;70:84–92.
29. Salman B, Mohammed H, Kherbeet AS. Numerical and experimental investigation of heat transfer enhancement in a microtube using nanofluids. Int Commun Heat Mass Transf. 2014;59:88–100.
30. Nimmagadda R, Venkatasubbaiah K. Experimental and multiphase analysis of nanofluids on the conjugate performance of micro-channel at low Reynolds numbers. Heat Mass Transf. 2017;53(6):2099–115.
31. Fadhillahanafi N, Leong K, Risby M. Stability and thermal conductivity characteristics of carbon nanotube based nanofluids. Int J Automot Mech Eng. 2013;8:1376.
32. Sadeghinezhad E, Togun H, Mehrali M, Nejad PS, Latibari ST, Abdulrazzaq T, et al. An experimental and numerical investigation of heat transfer enhancement for graphene nanoplatelets nanofluids in turbulent flow conditions. Int J Heat Mass Transf. 2015;81:41–51.
33. Manivannan S, Jeong IO, Ryu JH, Lee CS, Kim KS, Jang J, et al. Dispersion of single-walled carbon nanotubes in aqueous and organic solvents through a polymer wrapping functionalization. J Mater Sci Mater Electron. 2009;20(3):223–9.
34. Li W, Liang C, Zhou W, Qiu J, Zhou Z, Sun G, et al. Preparation and characterization of multiwalled carbon nanotube-supported platinum for cathode catalysts of direct methanol fuel cells. J Phys Chem B. 2003;107(26):6292–9.
35. Khavarian M, Chai S-P, Mohamed AR. Direct use of as-synthesized multi-walled carbon nanotubes for carbon dioxide reforming of methane for producing synthesis gas. Chem Eng J. 2014;257:200–8.
36. Duangthongsuk W, Wongwises S. Effect of thermophysical properties models on the predicting of the convective heat transfer coefficient for low concentration nanofluid. Int Commun Heat Mass Transf. 2008;35(10):1320–6.
37. Ghozatloo A, Azimi Maleki S, Shariaty-Niassar M, Morad RA. Investigation of nanoparticles morphology on viscosity of nanofluids and new correlation for prediction. J Nanostruct. 2015;5(2):161–8.
38. Xie H, Lee H, Youn W, Choi M. Nanofluids containing multiwalled carbon nanotubes and their enhanced thermal conductivities. J Appl Phys. 2003;94(8):4967–71.
39. Bergman TL, Incropera FP, DeWitt DP, Lavine AS. Fundamentals of heat and mass transfer. New York: Wiley; 2011.
40. Shah R, editor. Thermal entry length solutions for the circular tube and parallel plates. In: Third national heat mass transfer conference, Indian Institute of Technology, Bombay, India; 1975.
41. Taylor J. Introduction to error analysis, the study of uncertainties in physical measurements. Herndon: University Science Books; 1997.
42. Sara O, Barlay Ergu Ö, Arzutug M, Yapıcı S. Experimental study of laminar forced convective mass transfer and pressure drop in microtubes. Int J Therm Sci. 2009;48(10):1894–900.
43. Akhavan-Behabadi M, Shahidi M, Aligoodarz M, Ghazvini M. Experimental investigation on thermo-physical properties and overall performance of MWCNT-water nanofluid flow inside horizontal coiled wire inserted tubes. Heat Mass Transf. 2017;53(1):291–304.
44. Buongiorno J. Convective transport in nanofluids. J Heat Transf. 2006;128(3):240–50.
45. Liu D, Yu L. Single-phase thermal transport of nanofluids in a minichannel. J Heat Transf. 2011;133(3):031009.
46. Yang G, Wu J. Conjugate mixed convection in the entrance region of a symmetrically heated vertical channel with thick walls. Int J Therm Sci. 2015;98:245–54.
47. Li Z, He Y-L, Tang G-H, Tao W-Q. Experimental and numerical studies of liquid flow and heat transfer in microtubes. Int J Heat Mass Transf. 2007;50(17):3447–60.